Progress of Theoretical Physics, Vol. 75, No. 4, April 1986

Radiative Correction to $e^+e^- \to e^+e^-$ in the Electroweak Theory. II

—— *Corrected Elastic Cross Section and Positron Energy Spectrum* ——

Keijiro TOBIMATSU*) and Yoshimitsu SHIMIZU*

Department of Physics, Tokyo Metropolitan University, Tokyo 158
and
**National Laboratory for High Energy Physics, Tsukuba, Ibaraki 305*

(Received November 11, 1985)

Lowest order radiative correction to the Bhabha scattering, $e^+e^- \to e^+e^-$, is calculated in the standard electroweak theory. The real and hard photon emission is included so as to satisfy a realistic experimental condition. The corrected differential cross sections, $(d\sigma/d\Omega)_{\zeta<\zeta_c, q_{\pm 0}>E_{\rm th}}$, are given at $\sqrt{s}=70$, 93 and 150 GeV. An acollinearity angle cut, $\zeta_c=10^\circ$, and a threshold energy cut, $E_{\rm th}=20$ GeV, for the energies of the final e^+ and e^-, q_{+0} and q_{-0}, are imposed. The energy spectrum of scattered positron at fixed angle, $d\sigma/dq_{+0}d\cos\theta$, is also given which will be helpful for luminosity measurement of the colliding beams or background estimation due to radiative Bhabha scattering.

§ 1. Introduction

The Bhabha scattering, $e^+e^- \to e^+e^-$, has been one of the most interesting processes to be measured in high energy e^+e^- colliding beam experiments. Until now the observations obtained by PETRA[1] and PEP[2] seem to be consistent with the electroweak theory in its standard version. The effect due to Z^0 exchange has been clearly seen. In order to make the precise check of the theory, however, careful measurement around the Z^0 pole in the s-channel should be done. This is an important aim of the accelerators TRISTAN, SLC and LEP to be operated in the near future. The highest energy is expected even to exceed the mass of Z^0 boson. Further this process can be used to monitor the luminosity of colliding beams because of its large Coulomb cross section for the forward scattering.

In this paper we give corrected differential cross section $(d\sigma/d\Omega)_{\zeta<\zeta_c, q_{\pm 0}>E_{\rm th}}$ and $d\sigma/dq_{+0}d\cos\theta$. The complexity of the Bhabha scattering arises from the fact that the initial and final electrons (positrons) can easily emit real photons at the instance of scattering which in turn requires to include all relevant loop corrections to the lowest order amplitude in order to cancel the infrared singularity. In all the correction turns out to be order of ten percent. Thus the lowest order cross section is not sufficient when one is going to make realistic prediction. In a previous paper, Ref. 3) (referred to as I hereafter), we give various kinds of distributions for $e^+e^- \to e^+e^-\gamma$ assuming that we observe the photon as well as the final e^+ and e^-. When the final photon has a small energy, escapes into the beam pipe or is scattered unseparately close to the final e^+ or e^-, we cannot detect it so that we recognize this event as elastic one. Therefore the lowest order cross section should be modified by taking account of these corrections.

The radiative corrections to the process are usually divided into two classes, the virtual correction and the real photon emission. For the sake of convenience the latter is also divided into two, soft and hard photon emissions. The virtual correction requires

*) Present address: Meiji-gakuin University, Yokohama 244.

calculation of all one loop diagrams. These were given in Ref. 4) which studied the same problem for the μ-pair production. To fix the renormalization point we adopted the on-shell renormalization scheme reviewed comprehensively in Ref. 5). The main result obtained in Ref. 4) was that the correction to the axial vector part of eeZ^0 vertex is fairly large on the Z^0 pole in this scheme. This is also expected in the backward scattering of Bhabha, because the s-channel Z^0 pole dominates the cross section there. The soft photon emission cross section is obtaind in a well-known manner.

The lowest order radiative corrections to the Bhabha scattering have been studied by many authors in this decade. In Ref. 6) the complete calculation in the regime of QED was given including the contribution from hard photon emission. Reference 7) treated the same problem in the same way as Ref. 6) but at the energy of ADONE. In the standard electroweak theory, Consoli[8] was the first who calculated all one loop diagrams. He gave corrected cross section off the Z^0 pole within the soft photon approximation. After that the correction around the Z^0 pole was given in Ref. 9). The authors claimed that the pure weak contributions from Z^0-Z^0 or $W^{\pm}$-$W^{\mp}$ box diagrams or vertex diagram bridged by Z^0 boson are negligible compared with those involve photon internal line. Recently Böhm et al.[10] also calculated the corrections and gave $(d\sigma/d\Omega)_{k<k_c}$. In both Refs. 9) and 10), the contribution from the soft photon emission is exponentiated to include the higher order effectively and the cutoff is set to be $k_c=0.1\cdot E_{\text{beam}}$. Thus there is no work which accomodates with the full electroweak theory and hard photon emission. In this paper, we study the lowest order radiative correction throughly; we do not exponentiate the soft photon factor, but we take account of hard photon contribution obeying realistic experimental condition.

In the next section we give the corrected differential cross section, in the third section we discuss the positron energy spectrum and the last section contains conclusion and some comments.

§ 2. Differential cross section

The lowest order cross section including Z^0 exchange both in the s- and t-channels is given by

$$\left(\frac{d\sigma}{d\Omega}\right)_0=\frac{\alpha^2}{4s}\cdot(\tau_0^{(s)}+\tau_0^{(t)}+\tau_0^{(\text{int})}), \tag{1}$$

where

$$\tau_0^{(s)}=(1+\cos^2\theta)+\frac{2s(s-M_Z^2)}{D(s)}[C_V^2(1+\cos^2\theta)+2C_A^2\cos\theta]$$

$$+\frac{s^2}{D(s)}[(C_V^2+C_A^2)^2(1+\cos^2\theta)+8C_V^2C_A^2\cos\theta)],$$

$$\tau_0^{(t)}=2\left\{\frac{s^2}{t^2}\left(1+\cos^4\frac{\theta}{2}\right)+\frac{2s^2}{t(t-M_Z^2)}\left[(C_V^2-C_A^2)+(C_V^2+C_A^2)\cos^4\frac{\theta}{2}\right]\right.$$

$$\left.+\frac{s^2}{(t-M_Z^2)^2}\left[(C_V^2-C_A^2)^2+((C_V^2+C_A^2)^2+4C_V^2C_A^2)\cos^4\frac{\theta}{2}\right]\right\},$$

$$\tau_0^{(\mathrm{int})}=4\cos^4\frac{\theta}{2}\left\{\frac{s}{t}+\left(\frac{s^2(s-M_Z^2)}{tD(s)}+\frac{s}{t-M_Z^2}\right)(C_V^2+C_A^2)\right.$$
$$\left.+\frac{s^2(s-M_Z^2)}{D(s)(t-M_Z^2)}[(C_V^2+C_A^2)^2+4C_V^2C_A^2]\right\} \tag{2}$$

and

$$D(s)=(s-M_Z^2)^2+M_Z^2\Gamma_Z^2\,.$$

Here we neglect electron mass m_e but keep the finite decay width of Z^0 boson, Γ_Z. The square of the total energy and the scattering angle between final and initial positrons are denoted by s and θ, respectively. Parameters in which we need to fix the renormalization point are fermion masses, W boson mass M_W, Z^0 boson mass M_Z, Higgs mass M_H and fine structure constant α. By using M_Z and M_W, the vector and axial vector couplings at the eeZ^0 vertex, C_V and C_A, are expressed as

$$C_V=M_Z^2\left(3-\frac{4M_W^2}{M_Z^2}\right)/\left(4M_W\sqrt{M_Z^2-M_W^2}\right)\,,$$
$$C_A=M_Z^2/\left(4M_W\sqrt{M_Z^2-M_W^2}\right)\,. \tag{3}$$

Throughout this paper we take $M_Z=93$ GeV, $M_W=81$ GeV which are central values measured at CERN-S$\bar{\mathrm{P}}$PS[11] and $M_H=200$ GeV. The decay width of Z^0 boson is taken to be 2.28 GeV. This is obtained by naively calculating Z^0 decays into lepton and quark pairs of three generations (with top quark mass $m_t=40$ GeV). The width increases if one chooses lighter top quark mass or includes gluon emission from quarks as discussed in Ref. 12). The effect of this uncertainty will be shown later by varying the width from 2.28 to 2.7 GeV at $\sqrt{s}=93$ GeV. The lowest order cross sections at $\sqrt{s}=70$, 93 and 150 GeV are numerically given in Table I.

The soft photon emission cross section is given by

$$\left(\frac{d\sigma}{d\Omega}\right)_{\mathrm{soft}}=\left(\frac{d\sigma}{d\Omega}\right)_0\cdot R(k_c,\lambda)\,, \tag{4}$$

where $R(k_c,\lambda)$ is given by

$$R(k_c,\lambda)=R_{ii}+R_{ff}+R_{if}\,,$$
$$R_{ii}=\frac{2\alpha}{\pi}\cdot\left(\left(\log\left(\frac{s}{m_e^2}\right)-1\right)\log\left(\frac{2k_c}{\lambda}\right)-\frac{1}{4}\log^2\left(\frac{s}{m_e^2}\right)+\frac{1}{2}\log\left(\frac{s}{m_e^2}\right)-\frac{\pi^2}{6}\right),$$
$$R_{ff}=R_{ii}\,,$$
$$R_{if}=\frac{2\alpha}{\pi}\cdot\left(-4\log\left(\frac{\cos(\theta/2)}{\sin(\theta/2)}\right)\log\left(\frac{2k_c}{\lambda}\right)+\mathrm{Sp}\left(\cos^2\frac{\theta}{2}\right)-\mathrm{Sp}\left(\sin^2\frac{\theta}{2}\right)\right.$$
$$\left.-2\log\left(\frac{\cos(\theta/2)}{\sin(\theta/2)}\right)\cdot\log\left(\cos\frac{\theta}{2}\sin\frac{\theta}{2}\right)\right)$$

with the Spence function defined by

$$\mathrm{Sp}(z)=-\int_0^z\frac{dt}{t}\log(1-t)\,.$$

Here we introduced a ficititious photon mass λ and soft photon energy cut k_c. It should be noted that this formula is correct only for $k_c \ll \Gamma_z$ around the Z^0 pole, otherwise the resonance peak changes the form of radiative tail substantially. The formulas without this restriction can be found in the literature, for example, in Refs. 4) and 13). Also several authors gave exponentiated form of soft photon emission (Refs. 9) and 10)). However, in this paper, we choose k_c much smaller than the width, so that we use the simplest formula given above.

The hard photon emission cross section is defined by

$$\left(\frac{d\sigma}{d\Omega}\right)^{(1\gamma)}_{\zeta<\zeta_c, q_{\pm 0}>E_{\rm th}, k>k_c} = \frac{\alpha^3}{2s}\cdot\int \frac{k|\boldsymbol{q}_+|dkd\cos\theta_\gamma d\varphi_\gamma/2\pi}{W-k+kq_{+0}/|\boldsymbol{q}_+|\cos\theta}\cdot\tau^{(1\gamma)}. \tag{5}$$

Here $\tau^{(1\gamma)}$ is the matrix element squared for one photon emission process. We impose some kinematical cut for final particle configuration: The acollinearity angle ζ, defined as the complementary angle between final e^+ and e^-, should be less than the cut ζ_c and the energies of final e^+ and e^-, q_{+0} and q_{-0}, are to be larger than an energy cut $E_{\rm th}$. The kinematics for final three body state and how to integrate over the phase space incorporating various kinds of singularities are reviewed in I. We extensively used the symbolic manipulation program REDUCE[14] to get $\tau^{(1\gamma)}$ and multiple integration routines BASES[15] and VEGAS[16] to make phase space integration.

The one loop correction to the lowest order cross section is denoted by

$$\left(\frac{d\sigma}{d\Omega}\right)_{\rm virtual} = \left(\frac{d\sigma}{d\Omega}\right)_0\cdot\delta_V(\lambda). \tag{6}$$

The virtual correction consists of vertex, box and vacuum polarization. In the framework of QED these are given in Refs. 6) and 7). In the standard electroweak theory, all one loop diagrams are calculated in Ref. 10) but with vanishing Z^0 decay width. In this paper we follow the formulas given in Ref. 4). The explicit form of $\delta_V(\lambda)$ is so complicated and lengthy that we do not give it here. Combining the above equations 1)~6), we get the corrected cross section

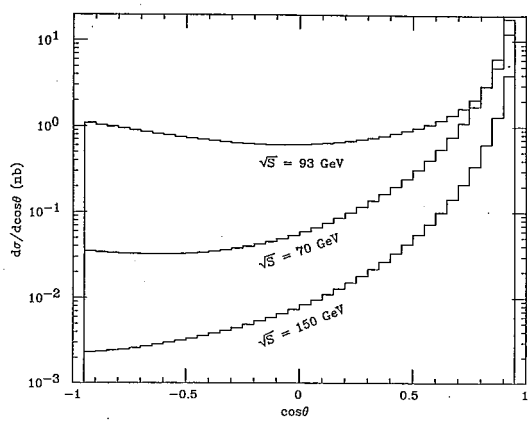

Fig. 1. The corrected differential cross sections $d\sigma/d\cos\theta$ at $\sqrt{s}=70$, 93 and 150 GeV.

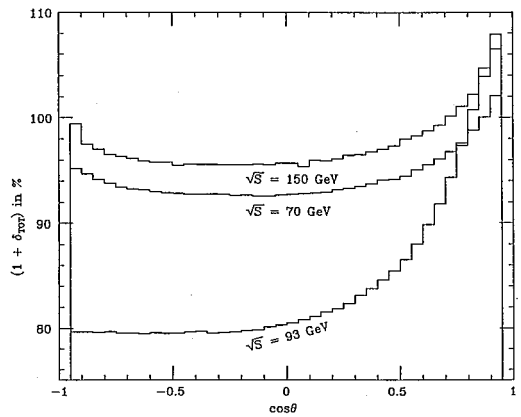

Fig. 2. The percentage radiative corrections $1+\delta_{TOT}$ at $\sqrt{s}=70$, 93 and 150 GeV.

$$\left(\frac{d\sigma}{d\Omega}\right)_{\zeta<\zeta_c, q_{\pm 0}>E_{\rm th}} = \left(\frac{d\sigma}{d\Omega}\right)_0 \cdot (1 + R(k_c, \lambda) + \delta_V(\lambda)) + \left(\frac{d\sigma}{d\Omega}\right)^{(1\gamma)}_{\zeta<\zeta_c, q_{\pm 0}>E_{\rm th}, k>k_c},$$

$$= \left(\frac{d\sigma}{d\Omega}\right)_0 \cdot (1 + \delta_{TOT}) . \tag{7}$$

Table I. Lowest order cross section $d\sigma^0/d\cos\theta$, analytic part of the radiative correction $\delta_A(k_c)$ with $k_c = 0.1$ GeV and total radiative correction in the range of $-0.925 \leqq \cos\theta \leqq 0.925$ at $\sqrt{s} = 70$, 93 and 150 GeV.

	$W=70$ GeV			$W=93$ GeV			$W=150$ GeV		
$\cos\theta$	Born (nb)	$\delta_A(\%)$	$\delta_{TOT}(\%)$	Born (nb)	$\delta_A(\%)$	$\delta_{TOT}(\%)$	Born (nb)	$\delta_A(\%)$	$\delta_{TOT}(\%)$
−0.925	3.680×10^{-2}	−113.1	−4.8±0.1	1.366	−109.3	−20.4±0.1	2.323×10^{-3}	−141.6	−0.6±0.1
−0.875	3.616×10^{-2}	−110.1	−5.3±0.1	1.300	−108.1	−20.4±0.1	2.402×10^{-3}	−137.8	−2.5±0.2
−0.825	3.561×10^{-2}	−108.2	−5.9±0.1	1.238	−107.3	−20.4±0.1	2.491×10^{-3}	−135.4	−3.0±0.1
−0.775	3.518×10^{-2}	−106.8	−6.2±0.1	1.180	−106.6	−20.3±0.1	2.591×10^{-3}	−133.5	−3.5±0.1
−0.725	3.486×10^{-2}	−105.6	−6.6±0.1	1.126	−106.1	−20.5±0.1	2.703×10^{-3}	−132.0	−3.7±0.1
−0.675	3.468×10^{-2}	−104.6	−6.7±0.1	1.075	−105.7	−20.5±0.1	2.830×10^{-3}	−130.7	−3.9±0.1
−0.625	3.466×10^{-2}	−103.8	−6.8±0.1	1.028	−105.3	−20.6±0.1	2.972×10^{-3}	−129.6	−4.1±0.1
−0.575	3.480×10^{-2}	−103.0	−7.0±0.1	9.845×10^{-1}	−104.9	−20.5±0.1	3.133×10^{-3}	−128.7	−4.2±0.1
−0.525	3.513×10^{-2}	−102.4	−7.1±0.1	9.449×10^{-1}	−104.6	−20.5±0.1	3.314×10^{-3}	−127.8	−4.2±0.1
−0.475	3.567×10^{-2}	−101.8	−7.2±0.1	9.091×10^{-1}	−104.2	−20.5±0.1	3.521×10^{-3}	−127.0	−4.5±0.1
−0.425	3.646×10^{-2}	−101.3	−7.3±0.1	8.771×10^{-1}	−103.9	−20.4±0.1	3.756×10^{-3}	−126.2	−4.4±0.1
−0.375	3.752×10^{-2}	−100.8	−7.3±0.1	8.488×10^{-1}	−103.7	−20.3±0.1	4.026×10^{-3}	−125.5	−4.5±0.1
−0.325	3.891×10^{-2}	−100.3	−7.2±0.1	8.244×10^{-1}	−103.4	−20.5±0.1	4.337×10^{-3}	−124.9	−4.4±0.1
−0.275	4.067×10^{-2}	−99.9	−7.3±0.1	8.038×10^{-1}	−103.1	−20.4±0.1	4.697×10^{-3}	−124.3	−4.5±0.1
−0.225	4.287×10^{-2}	−99.4	−7.4±0.1	7.871×10^{-1}	−102.8	−20.3±0.1	5.117×10^{-3}	−123.7	−4.5±0.1
−0.175	4.559×10^{-2}	−99.0	−7.3±0.1	7.743×10^{-1}	−102.6	−20.2±0.1	5.609×10^{-3}	−123.1	−4.5±0.1
−0.125	4.893×10^{-2}	−98.7	−7.4±0.1	7.654×10^{-1}	−102.3	−20.2±0.1	6.191×10^{-3}	−122.6	−4.4±0.1
−0.075	5.301×10^{-2}	−98.3	−7.4±0.1	7.606×10^{-1}	−102.1	−19.9±0.1	6.884×10^{-3}	−122.1	−4.5±0.1
−0.025	5.799×10^{-2}	−97.9	−7.3±0.1	7.599×10^{-1}	−101.8	−19.7±0.0	7.714×10^{-3}	−121.6	−4.3±0.1
0.025	6.407×10^{-2}	−97.5	−7.3±0.1	7.634×10^{-1}	−101.5	−19.5±0.0	8.718×10^{-3}	−121.1	−4.3±0.1
0.075	7.151×10^{-2}	−97.1	−7.2±0.1	7.712×10^{-1}	−101.3	−19.2±0.1	9.943×10^{-3}	−120.6	−4.6±0.8
0.125	8.065×10^{-2}	−96.8	−7.2±0.1	7.836×10^{-1}	−101.0	−18.9±0.1	1.145×10^{-2}	−120.1	−4.0±0.1
0.175	9.194×10^{-2}	−96.4	−7.1±0.1	8.007×10^{-1}	−100.7	−18.4±0.1	1.332×10^{-2}	−119.6	−4.1±0.1
0.225	1.060×10^{-1}	−96.0	−6.8±0.1	8.230×10^{-1}	−100.4	−18.1±0.1	1.568×10^{-2}	−119.1	−3.9±0.1
0.275	1.236×10^{-1}	−95.5	−6.7±0.1	8.508×10^{-1}	−100.1	−17.6±0.1	1.867×10^{-2}	−118.5	−3.6±0.1
0.325	1.460×10^{-1}	−95.1	−6.5±0.1	8.847×10^{-1}	−99.8	−16.9±0.1	2.253×10^{-2}	−118.0	−3.5±0.1
0.375	1.749×10^{-1}	−94.6	−6.3±0.1	9.257×10^{-1}	−99.5	−16.2±0.1	2.757×10^{-2}	−117.4	−3.2±0.1
0.425	2.126×10^{-1}	−94.2	−5.9±0.1	9.752×10^{-1}	−99.1	−15.4±0.1	3.429×10^{-2}	−116.8	−3.0±0.1
0.475	2.629×10^{-1}	−93.6	−5.8±0.1	1.035	−98.8	−14.5±0.1	4.343×10^{-2}	−116.2	−2.7±0.1
0.525	3.318×10^{-1}	−93.1	−5.5±0.1	1.109	−98.4	−13.5±0.1	5.616×10^{-2}	−115.5	−2.1±0.1
0.575	4.286×10^{-1}	−92.5	−4.9±0.1	1.201	−98.0	−12.0±0.1	7.442×10^{-2}	−114.8	−1.7±0.1
0.625	5.701×10^{-1}	−91.9	−4.5±0.1	1.321	−97.5	−10.2±0.1	1.016×10^{-1}	−114.0	−1.3±0.1
0.675	7.868×10^{-1}	−91.2	−3.9±0.1	1.487	−97.0	−8.2±0.1	1.440×10^{-1}	−113.2	−0.7±0.1
0.725	1.140	−90.4	−3.2±0.1	1.731	−96.4	−5.7±0.0	2.143×10^{-1}	−112.2	0.2±0.1
0.775	1.768	−89.5	−2.4±0.1	2.132	−95.6	−2.7±0.0	3.416×10^{-1}	−111.1	1.1±0.1
0.825	3.035	−88.4	−1.2±0.1	2.891	−94.7	0.8±0.1	6.026×10^{-1}	−109.7	2.2±0.1
0.875	6.180	−86.9	0.0±0.1	4.705	−93.4	4.7±0.1	1.261	−108.0	3.9±0.1
0.925	17.84	−84.9	2.1±0.1	11.31	−91.5	7.9±0.1	3.738	−105.5	6.5±0.1

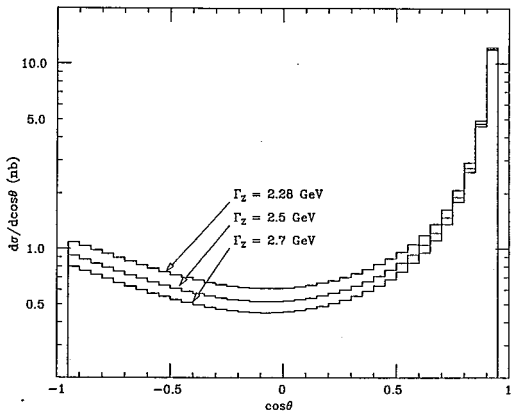

Fig. 3. The corrected differential cross sections $d\sigma/d\cos\theta$ at $\sqrt{s}=93$ GeV with $\Gamma_Z=2.28$, 2.5 and 2.7 GeV.

The left-hand side should not depend on the artificial cutoff λ and k_c. This is used for checking the numerical calculation. We changed k_c from 10^{-9} to 10^{-1} GeV and saw the final answer did not change. We show the corrected differential cross section in Fig. 1 and δ_{TOT} in Fig. 2 at $\sqrt{s}=70$, 93 and 150 GeV with $\zeta_c=10^\circ$ and $E_{\rm th}=20$ GeV. The scattering angle is limited in $|\cos\theta|\leqq 0.925$. The numerical results for percentage corrections to the lowest order cross section are summarized in Table I, where δ_A is the sum of corrections from virtual and soft photon emission ($k_c=0.1$ GeV). From Table I one can see that the contribution from real photon emission is almost cancelled by the virtual correction so that the net correction, δ_{TOT}, is rather small. This, in turn, implies that the correction is very sensitive to whether we include hard photon contribution or not. Thus the soft photon approximation is doubtful to give correct answer. By looking the energy dependence of the correction we find that it is large at $\sqrt{s}=93$ GeV while it is small for other energies far from Z^0 pole. Further the variance of corrected cross section at $\sqrt{s}=93$ GeV with the Z^0 width Γ_Z is shown in Fig. 3.

To check our calculation, we computed the correction of pure QED and compared it with the results given in Ref. 6). Further check was done. By switching off the t-channel contribution and replacing the final electron line by muon line, we calculated the correction to μ-pair production and compared it with that given in Ref. 17) in full electroweak theory. Excellent agreement within 0.1% was obtained for both cases. Next we compared our results with Table I of Ref. 9) under the same conditions as theirs. In this work they keep all loop diagrams obtained by attaching an internal photon line to the lowest order tree diagrams including Z^0 exchange (we refer these to 'partial' electroweak corrections). We got satisfactory agreement in the energy range from $\sqrt{s}=80$ GeV to 110 GeV. This proved that our results are correct as long as in the 'partial' electroweak theory. The check in the complete electroweak theory can be done by comparison with Fig. 2 of Ref. 10) which is given in the soft photon approximation. The angular dependence of the correction is qualitatively the same but we could not reproduce their results quantitatively. The difference between 'partial' and full electroweak corrections in the backward region seems to be too small in contrast to ours. Why the difference is so large on the Z^0 pole was discussed in detail in Ref. 4).

§ 3. Positron energy spectrum at fixed angle

In this section we discuss the positron energy spectrum at fixed angle, $d\sigma/dq_{+0}d\cos\theta$ and give the results at $\sqrt{s}=70$ GeV bearing in mind the TRISTAN. The final electron has a large probability to be scattered along the direction of initial electron, since the virtual photon exchanged in the t-channel is almost on shell (this is called t'-singularity

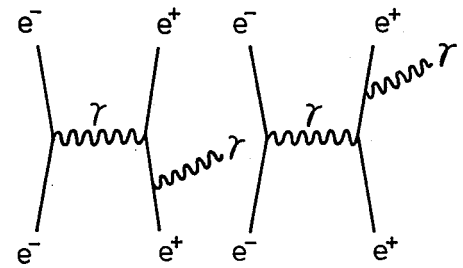

Fig. 4. Two Feynman diagrams which contain t'-singularity.

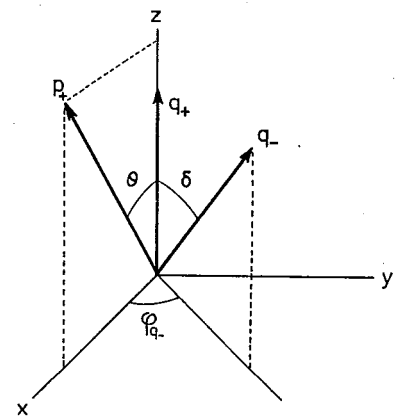

Fig. 5. The q'_+-frame.

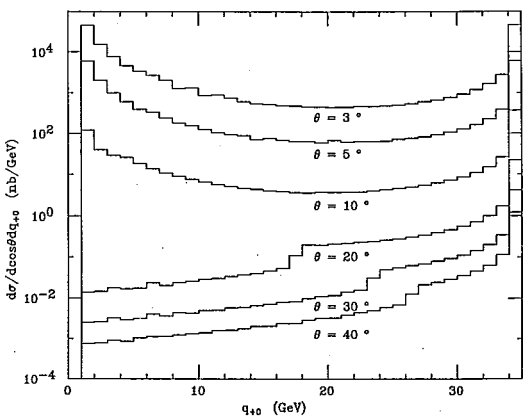

(a)

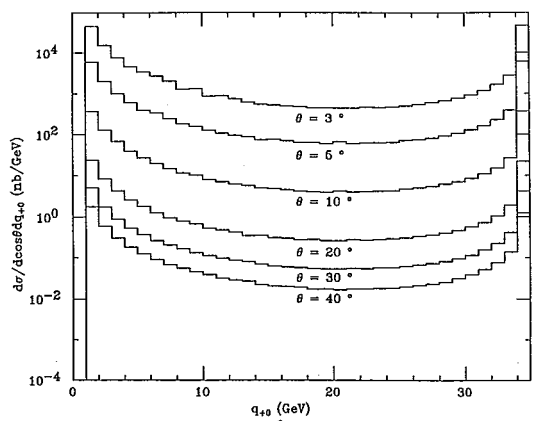

(b)

Fig. 6. The positron energy spectra $d\sigma/dq_{+0}d\cos\theta$ at $\theta=3°$, 5°, 10°, 20°, 30° and 40°. (a) $\zeta_c=10°$, (b) $\zeta_c=45°$.

in I) in this configuration. In this case the process can be well described by the real photon approximation. We have only to calculate two Feynman diagrams out of sixteen as depicted in Fig. 4. However, this approximation does not allow one to see how the cross section depends on whether the final electron is observed or not within the acollinearity angle cut so that we did not rely on this approximation but perform integration of $\tau^{(17)}$ without any simplification. This forces us to divide the integral region into two parts, one of which is a very narrow strip that contains the t'-singularity and the rest does not. In order to integrate over this t'-singularity effectively, we employ a new coordinate system q'_+-frame shown in Fig. 5. In this frame the cross section is given by

$$\frac{d\sigma}{dq_{+0}d\cos\theta}=\frac{\alpha^3}{4\pi s}\int\frac{|\boldsymbol{q}_+||\boldsymbol{q}_-|d\cos\delta d\varphi_{q-}}{W-q_{+0}+q_{-0}|\boldsymbol{q}_+|/|\boldsymbol{q}_-|\cos\delta}\tau^{(17)}. \tag{8}$$

When the integral region does not contain the sigularity we can safely use the formula in the q_+-frame discussed in detail in I.

The results are shown in Figs. 6 (a) and (b) for $\theta=3°$, 5°, 10°, 20°, 30° and 40°. Two sets of histograms (a) and (b) correspond to different acollinearity angle cut, $\zeta_c=10°$ for

(a) and $\zeta_c=45°$ for (b). We also impose an additional energy cut $q_{\pm 0}\geqq 1$ GeV. In the last bin which places at the maximum positron energy, we include the soft and virtual correction because the events in this bin cannot be distinguished from the elastic scattering. Comparing two histograms, one can see that both cross sections are almost the same at $\theta=3°$ and $\theta=5°$, but at $\theta=10°$ one finds a slight difference below $q_{+0}=20$ GeV. It reflects the fact that the cut $\zeta_c=45°$ involves the t'-singularity located at $\zeta=10^0=\theta$ whereas $\zeta_c=10°$ covers only half of the tail of the singularity. At larger θ the difference is clear because the condition $\zeta_c=10°$ of (a) excludes the singularity. It is noted that the cross sections have the minimum at $q_{+0}\sim 20$ GeV and become larger as q_{+0} decreases. This growing-up is just the effect of t'-singularity. The magnitude of the cross section at $\theta=3°$, $q_{+0}\leqq 1$ GeV is as large as $10^5\sim 10^6$ nb.

§ 4. Conclusion

The $O(\alpha^3)$ electroweak radiative corrections to Bhabha scattering have been completely calculated. The corrections amount to $-7.4\%\sim 2.1\%$, $-20.6\%\sim 7.9\%$ and $-4.5\%\sim 6.5\%$ at $\sqrt{s}=70$, 93 and 150 GeV, respectively, in the range $-0.925\leqq\cos\theta\leqq 0.925$ for $M_Z=93$ GeV, $M_W=81$ GeV, $\Gamma_Z=2.28$ GeV. Cross sections for different values of Z^0 width, $\Gamma_Z=2.5$ and 2.7 GeV at $\sqrt{s}=93$ GeV are also given. The results show sensitive dependence on the width. Further we calculated $d\sigma/dq_{+0}d\cos\theta$ at fixed θ which will be useful for luminosity measuring and background estimation.

At the end of conclusion we make a comment on our tedious computer work for this study. Total CPU time needed are about 100 hours by FACOM-M380 even for calculating 114 points of hard photon emission cross section for one k_c in Table I. One of the reasons for this unusually long CPU time for this kind of study is that the REDUCE output of $\tau^{(17)}$ is very long, containing about 4000 lines. In addition cancellation between real and virtual corrections requires the accuracy in 4 digits for Monte Carlo integration. This is, in general, not easy task by BASES or VEGAS. To get rid of this problem, we have only two ways: One is to use simpler $\tau^{(17)}$ than ours, as is given in Ref. 19). The other is to use faster machine, i.e., supercomputer with vector array processor. We are planning to develop the integral routine optimized to the supercomputer.[20] If the CPU time is made 20 times shorter than now, the work is manageable. This improvement is, more or less, inevitable because the calculation of radiative correction must be respeatedly done in a short time with various kinematical conditions in the course of e^+e^- colliding beam experiments.

Acknowledgements

A part of computer work has been financially supported by the Computer Center of Institute for Nuclear Study, University of Tokyo (INS). We would like to express our sincere gratitude to Dr. M. Yoshioka and members of High Energy Division at INS for their warm hospitality extended to us. One of us (K. T.) acknowledges Professor F. Takasaki, Professor T. Hirose and Professor T. Kobayashi for their continuous encouragement and guidance.

References

1) Cello Coll., H. -J. Behrend et al. Z. Phys. **C16** (1983), 301.
Jade Coll., W. Bartel et al, Z. Phys. **C19** (1983), 197.
Mark J Coll., B. Adeva et al., Phys. Rev. Lett. **48** (1982), 1701.
Tasso Coll., M. Althoff et al., Z. Phys. **C22** (1984), 13.
2) TPC Coll., H. Aihara et al., Z. Phys. **C27** (1985), 39; Phys. Rev. **D31** (1985), 2719.
MAC Coll., E. Fernandes et al., Phys. Rev. Lett. **54** (1985), 1620.
3) K. Tobimatsu and Y. Shimizu, Prog. Theor. Phys. **74** (1985), 567.
4) M. Igarashi, N. Nakazawa, T. Shimada and Y. Shimizu, Nucl. Phys. **B263** (1986), 347.
5) K-I. Aoki, Z. Hioki, R. Kawabe, M. Konuma and T. Muta, Prog. Theor. Phys. Suppl. No. 73 (1982), 1.
6) F. A. Berends, K. J. F. Gaemers and R. Gastmans, Nucl. Phys. **B68** (1974), 541.
See also F. A. Berends and R. Gastmans in *Electromagnetic Interactions of Hadron* ed. by A. Donnachie and G. Show (Plenum, 1978), vol. 2, p. 471.
7) E. Calva-Tellez, Phys. Rev. **D8** (1973), 3856.
8) M. Consoli, Nucl. Phys. **B160** (1979), 208.
9) M. Consoli, S. LO Presti and M. Greco, Phys. Lett. **B113** (1982), 415.
10) M. Böhm, A. Denner, W. Hollik and R. Sommer, Phys. Lett. **B144** (1984), 414.
11) G. Arnison et al., Phys. Lett. **126B** (1983), 398.
P. Bagnaia et al., Phys. Lett. **129B** (1983), 130.
G. Arnison et al., Phys. Lett. **129B** (1983), 273.
12) D. Albert, W. J. Marciano, D. Wyler and Z. Parsa, Nucl. Phys. **B166** (1980), 460.
13) F. A. Berends, R. Kleiss and S. Jadach, Nucl. Phys. **B202** (1982), 63.
14) A. C. Hearn, *REDUCE User's Mannual,* Version 3.0 (Rand Publication, 1983).
15) S. Kawabata, Comp. Phys. Comm. (to be published).
16) G. P. Lepage, J. Comp. Phys. **27** (1978), 192.
17) G. Passarino and M. Veltman, Nucl. Phys. **B160** (1979), 151.
18) F. A. Berends and R. Kleiss, Nucl. Phys. **B228** (1983), 537.
19) F. A. Berends, R. Gastmans and T. T. Wu, Preprint-KUL-TF-79/022, 1973.
20) S. Kawabata, private communication.